

A nonperturbative model for the strong running coupling

Yu.O. Belyakova^a and A.V. Nesterenko^b

^a*Department of Theoretical Physics, Faculty of Physics,
Moscow State University, Moscow 119991, Russian Federation*

^b*Bogoliubov Laboratory of Theoretical Physics,
Joint Institute for Nuclear Research, Dubna 141980, Russian Federation
E-mail: nesterav@theor.jinr.ru*

Abstract A nonperturbative model for the QCD invariant charge, which contains no low-energy unphysical singularities and possesses an elevated higher loop corrections stability, is developed. The static quark–antiquark potential is constructed by making use of the proposed model for the strong running coupling. The obtained result coincides with the perturbative potential at small distances and agrees with relevant lattice simulation data in the nonperturbative physically-relevant region. The developed approach yields a reasonable estimation of the value of the QCD scale parameter.

PACS: 11.15.Tk; 12.38.Aw; 12.39.Pn

Keywords: QCD running coupling; nonperturbative methods; quark confinement

1 Introduction

Theoretical description of hadron dynamics at large distances remains a crucial challenge of elementary particle physics for a long time. On the one hand, the asymptotic freedom of Quantum Chromodynamics (QCD) allows one to apply perturbation theory to the study of some “short-range” processes, for example, the high-energy hadronic reactions. On the other hand, the study of many phenomena related to the “long-range” dynamics (such as confinement of quarks, structure of the QCD vacuum, etc.) requires the nonperturbative methods.

In general, there is a variety of nonperturbative approaches to handle the strong interaction processes at low energies. For example, one can gain some hints about the low-energy hadron dynamics from lattice simulations [1], string models [2], sum rules [3, 4], dispersive (or analytic) approach to QCD [5–7], bag models [8], potential models [9–12]. In this paper we shall adhere the general lines

of the latter approach, that involves the construction of the QCD invariant charge which incorporates the perturbative and intrinsically nonperturbative features of the strong interaction.

The objective of this paper is to develop a nonperturbative model for the QCD invariant charge in the framework of potential approach. It is also of a primary interest to apply the proposed model to the construction of the static quark–antiquark potential and compare the obtained result with relevant lattice simulation data.

The layout of the paper is as follows. In Sect. 2 the model for the strong running coupling is formulated and its properties are discussed. Section 3 contains the construction of the potential of quark–antiquark interaction and its comparison with lattice data. In Conclusions (Sect. 4) the obtained results are summarized and further studies within the approach at hand are outlined. Appendix A contains the explicit expressions for the perturbative QCD β –function and strong running coupling up to the four–loop level. A brief description of the multi–valued Lambert W –function is given in App. B.

2 A nonperturbative strong running coupling

As it has been mentioned in the Introduction, the asymptotic freedom enables one to study the strong interaction processes at high energies within perturbative approach. However, the low–energy hadron dynamics entirely remains beyond the applicability range of perturbation theory. In what follows we shall adhere the general lines of the so–called potential approach [9–12] to the construction of the nonperturbative QCD invariant charge. Specifically, we shall construct the strong running coupling $\alpha(Q^2)$ that meets the requirements of the asymptotic freedom

$$\alpha(Q^2) \simeq \alpha_{\text{pert}}(Q^2), \quad Q^2 \rightarrow \infty, \quad (1)$$

and the infrared enhancement

$$\alpha(Q^2) \simeq \frac{4\pi}{\beta_0} \frac{\Lambda^2}{Q^2}, \quad Q^2 \rightarrow 0_+. \quad (2)$$

Here $\alpha_{\text{pert}}(Q^2)$ is the perturbative strong running coupling (see App. A), $\beta_0 = 11 - 2n_f/3$ denotes the first coefficient of the β –function perturbative expansion, n_f stands for the number of active quarks, $Q^2 \geq 0$ is the spacelike momentum transferred, and Λ denotes the QCD scale parameter. In terms of the renormalization group β –function

$$\frac{d \ln a(\mu^2)}{d \ln \mu^2} = \beta(a) \quad (3)$$

the conditions (1) and (2) can be rewritten as

$$\beta(a) \simeq \beta_{\text{pert}}(a), \quad a \rightarrow 0_+, \quad (4)$$

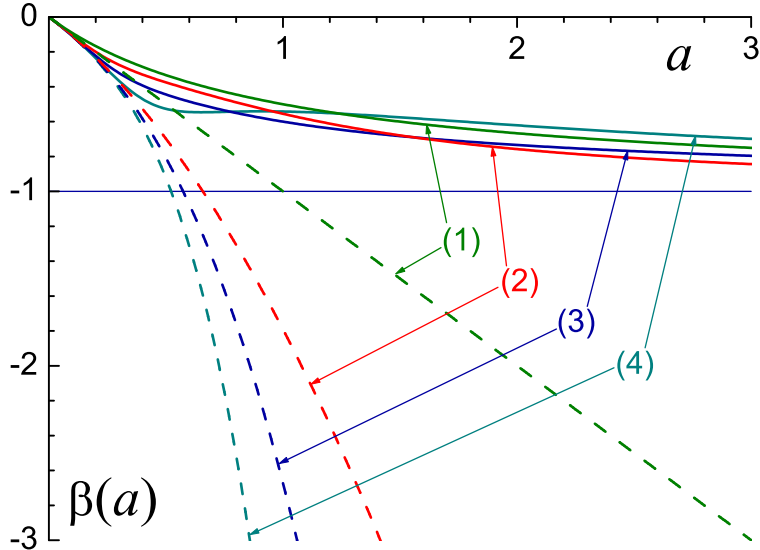


Figure 1: The β -function $\beta^{(\ell)}(a)$ (6) (solid curves) and the perturbative β -function $\beta_{\text{pert}}^{(\ell)}(a)$ (A.2) (dashed curves). The presented functions correspond to $n_f = 3$ active quarks. The numerical labels indicate the loop level.

and

$$\beta(a) \simeq -1, \quad a \rightarrow \infty, \quad (5)$$

respectively. In these equations $a(Q^2) = \alpha(Q^2)\beta_0/(4\pi)$ is the so-called ‘‘couplant’’.

One of the possible expressions for the β -function that satisfies conditions (4) and (5) reads

$$\beta^{(\ell)}(a) = \beta_{\text{pert}}^{(\ell)}(a) \frac{1 - \exp(-2/a)(1 - \ell^2/B_{\ell-1})}{1 + \ell^2 a^\ell}, \quad (6)$$

where $\beta_{\text{pert}}^{(\ell)}(a)$ is the ℓ -loop perturbative QCD β -function (A.2) and $B_n = \beta_n/\beta_0^{n+1}$ is the combination of the β -function expansion coefficients (see App. A). The plots of the function $\beta^{(\ell)}(a)$ (6) and the perturbative β -function (A.2) at ℓ -loop level ($\ell = 1, \dots, 4$) are presented in Figure 1. It is straightforward to verify that for large values of the couplant a the β -function (6) satisfies the aforementioned condition of linear confinement (5),

$$\beta^{(\ell)}(a) \simeq -1 + \mathcal{O}(a^{-1}), \quad a \rightarrow \infty, \quad (7)$$

whereas for the small values of a it coincides with the corresponding perturbative result (A.2):

$$\beta^{(\ell)}(a) \simeq \beta_{\text{pert}}^{(\ell)}(a) + \mathcal{O}(a^{\ell+1}), \quad a \rightarrow 0_+. \quad (8)$$

Additionally, β -function (6) admits the explicit integration of the renormalization group equation (3) at the one-loop level and eventually leads to the strong

running coupling $\alpha(Q^2)$ that contains no unphysical singularities at low energies and possesses an elevated stability with respect to the higher loop corrections.

For the beginning, let us consider the one-loop level ($\ell = 1$). In this case the β -function (6) takes a rather simple form, namely, $\beta^{(1)}(a) = -a/(1+a)$. The corresponding renormalization group equation for the QCD invariant charge reads

$$\frac{d \ln[a^{(1)}(\mu^2)]}{d \ln \mu^2} = -\frac{a^{(1)}(\mu^2)}{1+a^{(1)}(\mu^2)}. \quad (9)$$

After splitting the variables and integrating in finite limits, Eq. (9) takes the following form:

$$\frac{1}{a^{(1)}(Q^2)} - \ln[a^{(1)}(Q^2)] = \ln\left(\frac{Q^2}{\Lambda^2}\right), \quad (10)$$

where

$$\Lambda^2 = Q_0^2 \frac{\beta_0}{4\pi} \alpha^{(1)}(Q_0^2) \exp\left[-\frac{4\pi}{\beta_0} \frac{1}{\alpha^{(1)}(Q_0^2)}\right] \quad (11)$$

denotes the one-loop QCD scale parameter and Q_0^2 is the normalization point. Equation (10) can be solved explicitly in terms of the multi-valued Lambert W -function¹, namely,

$$\alpha^{(1)}(Q^2) = \frac{4\pi}{\beta_0} \frac{1}{W_0(z)}, \quad z = \frac{Q^2}{\Lambda^2}, \quad (12)$$

see also Refs. [14,15]. It is worthwhile to note here that only the principle branch of the Lambert W -function, $W_0(x)$, is physically meaningful herein. The plots of the couplant corresponding to the invariant charge (12), $a^{(1)}(Q^2) = 1/W_0(z)$, and the one-loop perturbative couplant (A.8), $a_{\text{pert}}^{(1)}(Q^2) = 1/\ln z$, are presented in Figure 2 (solid and dashed curves labeled “(1)”, respectively). The obtained strong running coupling (12) contains no low-energy unphysical singularities in the physical domain $Q^2 > 0$. By making use of the expansions (B.2) and (B.3) one can show that $\alpha^{(1)}(Q^2)$ (12) possesses the required infrared enhancement,

$$\alpha^{(1)}(Q^2) \simeq \frac{4\pi}{\beta_0} \left[\frac{1}{z} + 1 + \mathcal{O}(z) \right], \quad Q^2 \rightarrow 0_+, \quad (13)$$

and tends to the perturbative result (A.8) in the ultraviolet domain,

$$\alpha^{(1)}(Q^2) \simeq \frac{4\pi}{\beta_0} \left\{ \frac{1}{\ln z} + \mathcal{O}\left[\frac{\ln(\ln z)}{\ln^2 z}\right] \right\}, \quad Q^2 \rightarrow \infty. \quad (14)$$

It is worth mentioning here that the low-energy behaviour of the QCD invariant charge similar to that of Eq. (13) has also been discussed in Refs. [16–23].

Let us proceed now to the higher loop levels ($\ell > 1$). Here, the renormalization group equation (3) with the β -function (6) can only be integrated

¹The definition of the Lambert W -function and its properties are described in Ref. [13] and briefly overviewed in App. B.

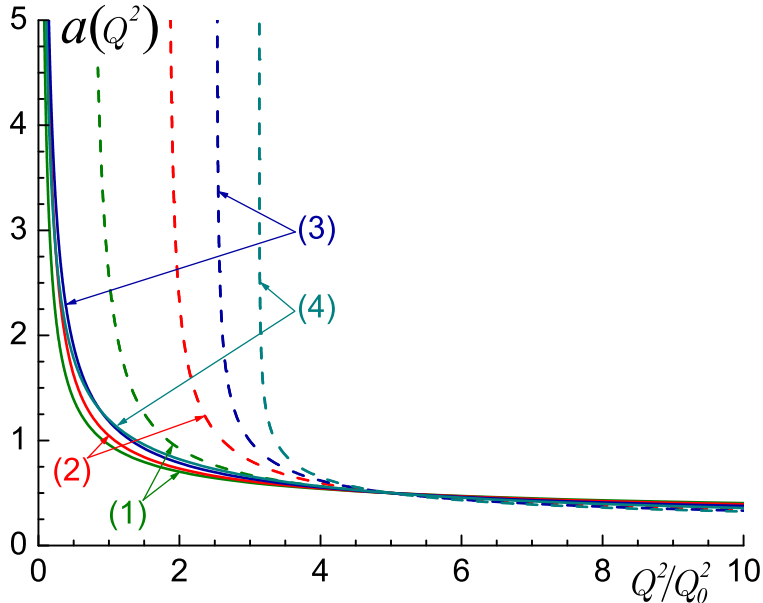


Figure 2: The ℓ -loop couplant $a^{(\ell)}(Q^2)$ corresponding to the β -function (6) (solid curves) and the perturbative couplant $a_{\text{pert}}^{(\ell)}(Q^2)$ (dashed curves). The presented functions are computed for $n_f = 3$ active quarks and normalized to the value $a(Q^2) = 1/2$ at $Q^2 = 5 Q_0^2$. The numerical labels indicate the loop level.

numerically. Nonetheless, the asymptotic behaviour of the ℓ -loop QCD invariant charge $\alpha^{(\ell)}(Q^2)$ corresponding to the β -function (6) can be found explicitly. Specifically, $\alpha^{(\ell)}(Q^2)$ possesses an enhancement in the infrared asymptotic,

$$\alpha^{(\ell)}(Q^2) \simeq \frac{4\pi}{\beta_0} \left[\frac{1}{z} + \mathcal{O}(z^0) \right], \quad Q^2 \rightarrow 0_+, \quad (15)$$

and coincides with perturbative strong running coupling $\alpha_{\text{pert}}^{(\ell)}(Q^2)$ (see App. A) in the ultraviolet asymptotic,

$$\alpha^{(\ell)}(Q^2) \simeq \alpha_{\text{pert}}^{(\ell)}(Q^2) + \mathcal{O} \left[\frac{\ln^\ell(\ln z)}{\ln^{\ell+1} z} \right], \quad Q^2 \rightarrow \infty. \quad (16)$$

The plots of the couplants $a^{(\ell)}(Q^2)$ and $a_{\text{pert}}^{(\ell)}(Q^2)$ at ℓ -loop level ($\ell = 1, \dots, 4$) are presented in Figure 2. As one may infer from this figure, the QCD invariant charge $\alpha^{(\ell)}(Q^2)$ possesses universal asymptotic behaviour and an elevated (with respect to perturbation theory) higher loop corrections stability in the intermediate energy range. It is worthwhile to note also that the proposed strong running coupling $\alpha(Q^2)$ is free of low-energy unphysical singularities.

3 Static quark–antiquark potential

Let us address now the construction of the static quark–antiquark potential $V(r)$. In the framework of the one-gluon exchange model $V(r)$ is related to the strong

running coupling $\alpha(Q^2)$ by the three-dimensional Fourier transformation

$$V(r) = -\frac{16\pi}{3} \int_0^\infty \frac{\alpha(Q^2)}{Q^2} \frac{\exp(i\mathbf{Q}\mathbf{r})}{(2\pi)^3} d\mathbf{Q}, \quad (17)$$

see, e.g., reviews [11,12] and references therein. Strictly speaking, this definition of the potential is justified for small distances ($r \lesssim 0.1$ fm) only. For example, the lowest-lying bound states of heavy quarks can be described by employing the perturbative² QCD [24]. However, at large distances ($r \gtrsim 0.5$ fm), which play the crucial role in hadron spectroscopy, the perturbative approach becomes inapplicable due to the infrared unphysical singularities (such as the Landau pole) of the strong running coupling $\alpha_{\text{pert}}(Q^2)$. Nonetheless, the potential (17), being constructed with the invariant charge $\alpha(Q^2)$ which embodies both perturbative and nonperturbative inputs, has proved to be successful in the description of meson spectrum (see, e.g., reviews [11,12] and references therein for the details).

In this paper, for the construction of the static potential of quark-antiquark interaction we shall use the invariant charge (12). After integration over angular variables, Eq. (17) in this case takes the form

$$V(r) = -\frac{32}{3\beta_0} \Lambda \int_0^\infty a(p^2\Lambda^2) \frac{\sin(pR)}{pR} dp, \quad (18)$$

where $p = Q/\Lambda$, $R = r\Lambda$, and $a(p^2\Lambda^2) = 1/W_0(p^2)$. The integral (18) diverges at the lower limit, that is a common feature of the models of such kind (discussion of this issue can be found in Ref. [11]). To regularize Eq. (18) it is convenient to split the couplant (12) into singular and regular parts (see also Eq. (13)):

$$a(p^2\Lambda^2) = a_1(p^2) + a_2(p^2), \quad (19)$$

where

$$a_1(p^2) = \frac{1}{p^2}, \quad a_2(p^2) = \frac{1}{W_0(p^2)} - \frac{1}{p^2}. \quad (20)$$

Then, the potential (18) takes the following form:

$$V(r) = \frac{8\pi}{3\beta_0} \Lambda \left[U_1(R) + U_2(R) \right], \quad (21)$$

where

$$U_i(R) = -\frac{1}{R} \frac{4}{\pi} \int_0^\infty a_i \left(\frac{x^2}{R^2} \right) \frac{\sin x}{x} dx, \quad i = 1, 2 \quad (22)$$

²The leading short-distance nonperturbative effect due to the gluon condensate has also been accounted for in Ref. [24].

are the dimensionless parts of the potential and $x = Qr$. The function $U_1(R)$ diverges and requires regularization, whereas $U_2(R)$ is regular and can be computed numerically.

To regularize function $U_1(R)$ we shall employ the method similar to that of used in Ref. [16]. Specifically, in terms of auxiliary function

$$I(t) = \int_0^{\infty} x^t \sin x \, dx \quad (23)$$

the singular part of the potential (21) reads

$$U_1(R) = -\frac{4}{\pi} I(-3) R. \quad (24)$$

The integral on the right hand side of Eq. (23) exists for $0 \leq |\operatorname{Re}(t+1)| < 1$ (see, e.g., Ref. [25]). Nonetheless, Eq. (23) can be analytically continued to the entire³ complex t -plane. This continuation is given by

$$I(t) = \sqrt{\pi} 2^t \frac{\Gamma(1+t/2)}{\Gamma((1-t)/2)} \quad (25)$$

and plays the role of regularization of Eq. (24), see also Refs. [6, 16]. In this case $I(-3) = -\pi/4$, that results in $U_1(R) = R$.

Thus, the static quark–antiquark potential (18) takes the following form:

$$V(r) = V_0 + \frac{8\pi}{3\beta_0} \Lambda \left[R - \frac{1}{R} \frac{4}{\pi} \int_0^{\infty} a_2 \left(\frac{x^2}{R^2} \right) \frac{\sin x}{x} \, dx \right], \quad R = \Lambda r, \quad (26)$$

where V_0 is an additive self–energy constant and $a_2(p^2)$ is given by Eq. (20). At small distances this potential possesses the standard behaviour determined by the asymptotic freedom

$$V(r) \simeq \frac{8\pi}{3\beta_0} \Lambda \frac{1}{R \ln R}, \quad r \rightarrow 0, \quad (27)$$

whereas at large distances potential (26) proves to be linearly rising

$$V(r) \simeq \frac{8\pi}{3\beta_0} \Lambda R, \quad r \rightarrow \infty, \quad (28)$$

implying the confinement of quarks. It is straightforward to verify that the potential (26) satisfies also the so–called concavity condition

$$\frac{dV(r)}{dr} > 0, \quad \frac{d^2V(r)}{dr^2} \leq 0, \quad (29)$$

which is a general property of the gauge theories (see Ref. [26] for the details).

³Except for the singular points of the right hand side of Eq. (25), such as $t = -2N$, with $N = 1, 2, 3, \dots$ being a natural number.

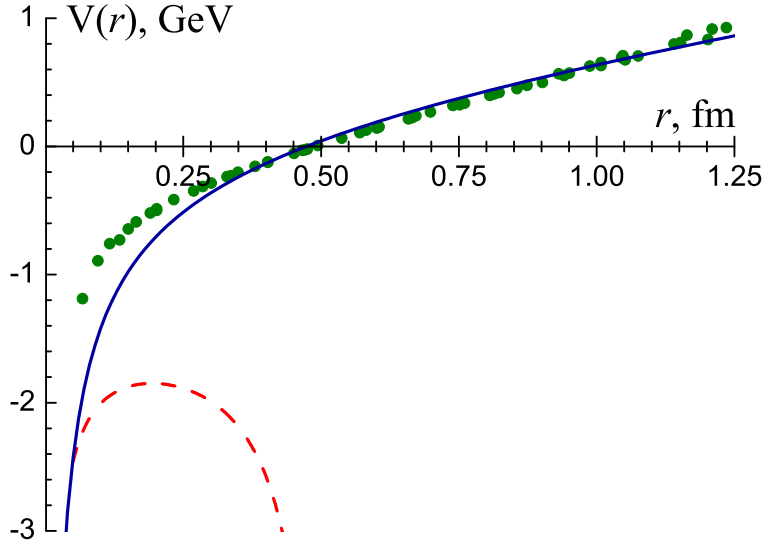


Figure 3: The quark–antiquark potential $V(r)$ (Eq. (26), solid curve) and the lattice simulation data [27] (\bullet). The dashed curve denotes the relevant perturbative result (27). The values of the parameters: $\Lambda = 375$ MeV, $V_0 = 315$ MeV, $n_f = 3$.

The comparison of the quark–antiquark potential (26) with relevant lattice simulation data [27] is shown in Figure 3. The fit has been performed with the use of the least square method, the scale parameter Λ and V_0 being the varied parameters in Eq. (26). The estimation of the value of Λ in the course of this comparison gives $\Lambda = (375 \pm 40)$ MeV (this value corresponds to the one–loop level with $n_f = 3$ active quarks). As one may infer from Figure 3, in the nonperturbative physically–relevant range $0.3 \text{ fm} \lesssim r \lesssim 1.2 \text{ fm}$, in which the average quark separations $\sqrt{\langle r^2 \rangle}$ for quarkonia sits [28], the quark–antiquark potential (26) reproduces the lattice data [27] fairly well. At the same time, in the region $r \lesssim 0.05 \text{ fm}$ the derived potential coincides with the perturbative⁴ result (27). The difference between the lattice data and the expression (26) in the intermediate range $0.05 \text{ fm} \lesssim r \lesssim 0.3 \text{ fm}$ may be explained by the presence of additional nonperturbative contributions at these distances (see, e.g., Ref. [30]), but the detailed investigation of this issue is beyond the scope of the paper.

4 Conclusions

A nonperturbative model for the QCD invariant charge is developed. The proposed strong running coupling is free of low–energy unphysical singularities and embodies the asymptotic freedom with infrared enhancement in a single expression. The model at hand possesses an elevated (with respect to perturbation theory) higher loop corrections stability in the intermediate energy range. The

⁴The applicability range of the perturbative quark–antiquark potential has been discussed in Refs. [10, 29].

static quark–antiquark potential is constructed by making use of the proposed model for the strong running coupling. The obtained result coincides with the perturbative potential at small distances and agrees with relevant lattice simulation data in the nonperturbative physically–relevant region. The developed approach yields a reasonable estimation of the value of the QCD scale parameter.

In further studies it would undoubtedly be interesting to compute the meson spectrum by making use of the derived quark–antiquark potential as well as to apply the developed model for the QCD invariant charge to the analysis of other strong interaction processes.

Acknowledgments

Authors are grateful to Professor G.S. Bali for supplying the relevant lattice simulation data and useful comments.

A The QCD β –function and running coupling within perturbation theory

The QCD invariant charge $\alpha(Q^2)$ is the solution of the renormalization group equation

$$\frac{d \ln[a(\mu^2)]}{d \ln \mu^2} = \beta(a), \quad (\text{A.1})$$

where $a(Q^2) = \alpha(Q^2)\beta_0/(4\pi)$ is the so–called “couplant”. For small values of the running coupling the right hand side of Eq. (A.1) is usually approximated by the power series, namely,

$$\beta(a) \simeq \beta_{\text{pert}}^{(\ell)}(a) = - \sum_{n=0}^{\ell-1} B_n [a^{(\ell)}(\mu^2)]^{n+1}, \quad a \rightarrow 0_+, \quad (\text{A.2})$$

where $\ell = 1, 2, 3, \dots$ denotes the loop level and $B_n = \beta_n/\beta_0^{n+1}$ is the combination of the QCD β –function perturbative expansion coefficients:

$$\beta_0 = 11 - \frac{2}{3} n_f, \quad (\text{A.3})$$

$$\beta_1 = 102 - \frac{38}{3} n_f, \quad (\text{A.4})$$

$$\beta_2 = \frac{2857}{2} - \frac{5033}{18} n_f + \frac{325}{54} n_f^2, \quad (\text{A.5})$$

$$\begin{aligned} \beta_3 = & \frac{149753}{6} + 3564 \zeta(3) - \left[\frac{1078361}{162} + \frac{6508}{27} \zeta(3) \right] n_f \\ & + \left[\frac{50065}{162} + \frac{6472}{81} \zeta(3) \right] n_f^2 + \frac{1093}{729} n_f^3. \end{aligned} \quad (\text{A.6})$$

In these equations n_f stands for the number of active quarks and $\zeta(x)$ denotes the Riemann ζ -function, $\zeta(3) \simeq 1.202$ (see, e.g., Ref. [25]). The one- and two-loop coefficients (β_0 and β_1) are scheme-independent, whereas the expressions given for β_2 and β_3 are calculated in the $\overline{\text{MS}}$ subtraction scheme (see papers [31–34] and references therein for the details). The plots of the β -function (A.2) are presented in Figure 1 (dashed curves).

The renormalization group equation corresponding to the perturbative β -function (A.2),

$$\frac{d \ln[a_{\text{pert}}^{(\ell)}(\mu^2)]}{d \ln \mu^2} = \beta_{\text{pert}}^{(\ell)}(a), \quad (\text{A.7})$$

can be solved explicitly at one- and two-loop levels ($\ell = 1, 2$), namely,

$$a_{\text{pert}}^{(1)}(Q^2) = \frac{1}{\ln z}, \quad z = \frac{Q^2}{\Lambda^2}, \quad (\text{A.8})$$

$$\begin{aligned} a_{\text{pert}}^{(2)}(Q^2) &= -\frac{B_1^{-1}}{1 + W_{-1}\left\{-\exp\left[-(1 + B_1^{-1} \ln z)\right]\right\}} \\ &\simeq \frac{1}{\ln z} - B_1 \frac{\ln(\ln z)}{\ln^2 z}, \quad Q^2 \rightarrow \infty \end{aligned} \quad (\text{A.9})$$

(see also Refs. [35]). In Eq. (A.9) $W_k(x)$ stands for the so-called Lambert W -function (see App. B for the details). Starting from the three-loop level, the exact solution to the perturbative renormalization group equation (A.7) can not be expressed in terms of known functions. Nonetheless, for $\ell \geq 3$ Eq. (A.7) can be solved iteratively, that eventually leads to

$$\begin{aligned} a_{\text{pert}}^{(3)}(Q^2) &\simeq \frac{1}{\ln z} - B_1 \frac{\ln(\ln z)}{\ln^2 z} \\ &\quad + \frac{1}{\ln^3 z} \left\{ B_1^2 \left[\ln^2(\ln z) - \ln(\ln z) - 1 \right] + B_2 \right\}, \end{aligned} \quad (\text{A.10})$$

$$\begin{aligned} a_{\text{pert}}^{(4)}(Q^2) &\simeq \frac{1}{\ln z} - B_1 \frac{\ln(\ln z)}{\ln^2 z} \\ &\quad + \frac{1}{\ln^3 z} \left\{ B_1^2 \left[\ln^2(\ln z) - \ln(\ln z) - 1 \right] + B_2 \right\} \\ &\quad + \frac{1}{\ln^4 z} \left\{ B_1^3 \left[-\ln^3(\ln z) + \frac{5}{2} \ln^2(\ln z) \right. \right. \\ &\quad \left. \left. + 2 \ln(\ln z) - \frac{1}{2} \right] - 3B_1 B_2 \ln(\ln z) + \frac{1}{2} B_3 \right\}. \end{aligned} \quad (\text{A.11})$$

It is worth noting here that the presented in Figure 2 plots of the ℓ -loop perturbative couplant $a_{\text{pert}}^{(\ell)}(Q^2)$ ($\ell = 1, \dots, 4$) correspond to exact solutions of the renormalization group equation (A.7).

B The Lambert W -function

The Lambert W -function is defined as a multi-valued function $W_k(x)$, which satisfies the equation

$$W_k(x) \exp[W_k(x)] = x, \quad (\text{B.1})$$

where k denotes the branch index. Only two branches of this function, namely, $W_0(x)$ (the principal branch) and $W_{-1}(x)$, take real values (see Figure 4), whereas the other branches take imaginary values. For the branches $W_0(x)$ and $W_{-1}(x)$ the following expansions hold:

$$W_0(x) = \ln x - \ln(\ln x) + \mathcal{O}\left[\frac{\ln(\ln x)}{\ln x}\right], \quad x \rightarrow \infty, \quad (\text{B.2})$$

$$W_0(x) = x - x^2 + \mathcal{O}(x^3), \quad x \rightarrow 0, \quad (\text{B.3})$$

$$W_{-1}(-x) = \ln x + \mathcal{O}(\ln |\ln x|), \quad x \rightarrow 0_+, \quad (\text{B.4})$$

$$W_{-1}\left(-\frac{1}{e} + x\right) = -1 - \sqrt{2ex} + \mathcal{O}(x), \quad x \rightarrow 0_+, \quad (\text{B.5})$$

where $e \simeq 2.71828$ denotes the base of the natural logarithm. The detailed description of the Lambert W -function and its properties can be found in Ref. [13].

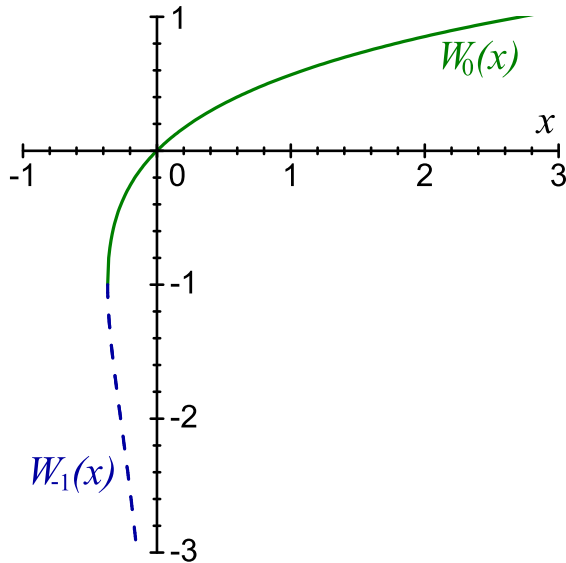


Figure 4: Two real branches of the Lambert W -function (B.1): $W_0(x)$ (solid curve) and $W_{-1}(x)$ (dashed curve).

References

- [1] C. Gatteringer and C.B. Lang, *Lect. Notes Phys.* **788**, 1 (2010); H.J. Rothe, *World Sci. Lect. Notes Phys.* **74**, 1 (2005).

- [2] B.M. Barbashov and V.V. Nesterenko, *Introduction to the Relativistic String Theory*, World Scientific, Singapore, 264 p. (1990).
- [3] M.A. Shifman, A.I. Vainshtein, and V.I. Zakharov, *Nucl. Phys. B* **147**, 385 (1979); **147**, 448 (1979).
- [4] L.J. Reinders, H. Rubinstein, and S. Yazaki, *Phys. Rept.* **127**, 1 (1985); S. Narison, *Nucl. Phys. B (Proc. Suppl.)* **164**, 225 (2007); arXiv:1010.1959 [hep-ph].
- [5] D.V. Shirkov and I.L. Solovtsov, *Theor. Math. Phys.* **150**, 132 (2007) [*Teor. Mat. Fiz.* **150**, 152 (2007)].
- [6] A.V. Nesterenko, *Int. J. Mod. Phys. A* **18**, 5475 (2003).
- [7] G. Cvetič and C. Valenzuela, *Braz. J. Phys.* **38**, 371 (2008).
- [8] P. Hasenfratz and J. Kuti, *Phys. Rept.* **40**, 75 (1978); S.L. Adler and T. Piran, *Rev. Mod. Phys.* **56**, 1 (1984).
- [9] W. Celmaster and F.S. Henyey, *Phys. Rev. D* **18**, 1688 (1978); J.L. Richardson, *Phys. Lett. B* **82**, 272 (1979). R. Levine and Y. Tomozawa, *Phys. Rev. D* **19**, 1572 (1979); **21**, 840 (1980).
- [10] W. Buchmüller, G. Grunberg, and S.-H. H. Tye, *Phys. Rev. Lett.* **45**, 103 (1980); **45**, 587(E) (1980); W. Buchmüller and S.-H. H. Tye, *Phys. Rev. D* **24**, 132 (1981).
- [11] W. Lucha, F.F. Schoberl, and D. Gromes, *Phys. Rept.* **200**, 127 (1991); W. Lucha and F.F. Schoberl, arXiv:hep-ph/9601263.
- [12] N. Brambilla and A. Vairo, arXiv:hep-ph/9904330.
- [13] R.M. Corless, G.H. Gonnet, D.E.G. Hare, D.J. Jeffrey, and D.E. Knuth, *Adv. Comput. Math.* **5**, 329 (1996); D.J. Jeffrey, D.E.G. Hare, and R.M. Corless, *Math. Scient.* **21**, 1 (1996).
- [14] Yu.O. Belyakova, *Proc. Int. Conf. Lomonosov-2009* (Moscow, Russia, 2009). Ed. by N.N. Sysoev. Moscow State University, p. 215 (2009).
- [15] Yu.O. Belyakova, *Proc. Int. Conf. Lomonosov-2010* (Moscow, Russia, 2010). Ed. by N.N. Sysoev. Moscow State University, Vol. 2, p. 155 (2010).
- [16] A.V. Nesterenko, *Phys. Rev. D* **62**, 094028 (2000); **64**, 116009 (2001).
- [17] A.V. Nesterenko, *Nucl. Phys. B (Proc. Suppl.)* **133**, 59 (2004); *Int. J. Mod. Phys. A* **19**, 3471 (2004).

- [18] A.V. Nesterenko, *Proc. 4th Int. Conf. on Quark Confinement and the Hadron Spectrum* (Vienna, Austria, 2000). Ed. by W. Lucha and K.M. Maung. World Scientific, p. 255 (2002); arXiv:hep-ph/0010257.
- [19] A.V. Nesterenko, *Proc. 5th Int. Conf. on Quark Confinement and the Hadron Spectrum* (Gargnano, Italy, 2002). Ed. by N. Brambilla and G. Proserpi. World Scientific, p. 288 (2003); arXiv:hep-ph/0210122.
- [20] A.C. Aguilar, A.V. Nesterenko, and J. Papavassiliou, *J. Phys. G* **31**, 997 (2005).
- [21] A.I. Alekseev and B.A. Arbuzov, *Mod. Phys. Lett. A* **13**, 1747 (1998); **20**, 103 (2005); *Phys. Atom. Nucl.* **61**, 264 (1998) [*Yad. Fiz.* **61**, 314 (1998)].
- [22] P.A. Raczka, *Nucl. Phys. B (Proc. Suppl.)* **164**, 211 (2007); arXiv:hep-ph/0602085; arXiv:hep-ph/0608196.
- [23] V.V. Kiselev, A.E. Kovalsky, and A.I. Onishchenko, *Phys. Rev. D* **64**, 054009 (2001).
- [24] S. Titard and F.J. Yndurain, *Phys. Rev. D* **49**, 6007 (1994); **51**, 6348 (1995).
- [25] I.S. Gradshteyn and I.M. Ryzhik, *Table of Integrals, Series, and Products*, ed. by A. Jeffrey (Academic, London, 1994).
- [26] E. Seiler, *Phys. Rev. D* **18**, 482 (1978); C. Bachas, *ibid. D* **33**, 2723 (1986).
- [27] G.S. Bali *et al.*, (SESAM and T χ L Collaborations), *Phys. Rev. D* **62**, 054503 (2000).
- [28] G.S. Bali, K. Schilling, and A. Wachter, *Phys. Rev. D* **56**, 2566 (1997); G.S. Bali and P. Boyle, *ibid. D* **59**, 114504 (1999).
- [29] M. Peter, *Phys. Rev. Lett.* **78**, 602 (1997); *Nucl. Phys. B* **501**, 471 (1997); K. Hagiwara, A.D. Martin, and A.W. Peacock, *Z. Phys. C* **33**, 135 (1986).
- [30] R. Akhoury and V.I. Zakharov, *Phys. Lett. B* **438**, 165 (1998); G.S. Bali, *ibid. B* **460**, 170 (1999); T. Lee, *Phys. Rev. D* **67**, 014020 (2003).
- [31] D.J. Gross and F. Wilczek, *Phys. Rev. Lett.* **30**, 1343 (1973); H.D. Politzer, *ibid.* **30**, 1346 (1973).
- [32] W.E. Caswell, *Phys. Rev. Lett.* **33**, 244 (1974); D.R.T. Jones, *Nucl. Phys. B* **75**, 531 (1974); E. Egorian and O.V. Tarasov, *Theor. Math. Phys.* **41**, 863 (1979) [*Teor. Mat. Fiz.* **41**, 26 (1979)].
- [33] O.V. Tarasov, A.A. Vladimirov, and A.Yu. Zharkov, *Phys. Lett. B* **93**, 429 (1980); S.A. Larin and J.A.M. Vermaseren, *ibid.* **303**, 334 (1993).

- [34] T. van Ritbergen, J.A.M. Vermaseren, and S.A. Larin, *Phys. Lett. B* **400**, 379 (1997); K.G. Chetyrkin, B.A. Kniehl, and M. Steinhauser, *Phys. Rev. Lett.* **79**, 2184 (1997).
- [35] E. Gardi, G. Grunberg, and M. Karliner, *JHEP* **9807**, 007 (1998); B.A. Magradze, arXiv:hep-ph/9808247.